Journal of Nuclear Medicine, published on May 5, 2016 as doi:10.2967/jnumed.116.173948

Variation of Specific Activities of Ga-68-Aquibeprin and Ga-68-Avebetrin Enables Selective PET-Imaging of Different Expression Levels of Integrins $\alpha_5\beta_1$ and $\alpha_v\beta_3$

Johannes Notni[1], Katja Steiger[2], Frauke Hoffmann[1], Dominik Reich[1], Markus Schwaiger[3], Horst Kessler[4], Hans-Jürgen Wester[1]

1 Lehrstuhl für Pharmazeutische Radiochemie, Technische Universität München, Garching, Germany

2 Institute of Pathology, Technische Universität München, Munich, Germany

3 Department of Nuclear Medicine,Technische Universität München, Munich, Germany

4 Institute for Advanced Study and Center of Integrated Protein Science, Department Chemie, Technische Universität München, Munich, Germany

Corresponding Author:

Johannes Notni

Lehrstuhl für Pharmazeutische Radiochemie

Technische Universität München

Walther-Meissner-Strasse 3

D-85748 Garching

Germany

email address: johannes.notni@tum.de

tel: +498928910266 / fax: +498928912204

Running title: Specific Activity in Integrin PET

Word count: 5393

ABSTRACT

Ga-68-Aquibeprin and Ga-68-Avebetrin are tracers for selective in-vivo mapping of integrins $\alpha_5\beta_1$ and $\alpha_v\beta_3$, respectively, by positron emission tomography (PET). As both tracers exhibit very high affinity to their respective targets, the aim of this study was to investigate the influence of the specific activity of preparations of both tracers on in vivo imaging results. **Methods:** Fully automated Ga-68 labelling of 0.3 nmol of Aquibeprin or Avebetrin was done using buffered eluate fractions (600–800 MBq, pH 2) of a SnO_2-based generator, affording the radiopharmaceuticals with specific activities >1,000 MBq/nmol. Lower values ranging from 150 to 0.4 MBq/nmol were adjusted by addition of inactive compound (approx. 0.15 to 50 nmol) to the injected activity (~ 20 MBq for PET, 5–7 MBq for biodistribution). For in vivo experiments, 6–12 weeks old, female SCID mice bearing M21 xenografts (human melanoma, expressing both integrins $\alpha_5\beta_1$ and $\alpha_v\beta_3$) were used. The expression density of integrin β_3 was determined by immunohistochemistry on paraffine slices. **Results:** For mass doses (specific activities) of < 20 pmol (>1,000 MBq/nmol) and 1 nmol (20 MBq/nmol) per mouse, respectively, uptakes of Ga-68-Aquibeprin / Ga-68-Avebetrin in M21 tumors dropped from 5.3 / 3.5 % ID/g to 3.0 / 2.4 % ID/g, respectively. Applying < 20 pmol, high uptakes of Ga-68-Aquibeprin in eyes (4.5 % ID/g) or Ga-68-Avebetrin in adrenals (25.9 % ID/g), respectively, were found, which were reduced by 90 and 65% (0.44 and 6.2 % ID/g, respectively), for doses of 1 nmol. Highest tumor-to-tissue ratios were observed both in ex-vivo biodistribution and PET for comparably large doses, e.g., 6 nmol (0.65 mg/kg) Ga-68-Aquibeprin per

mouse (3.5 MBq/nmol). **Conclusions:** Presumably owing to their high affinities, Ga-68-Aquibeprin and Ga-68-Avebetrin allow for selective addressing of target sites with different integrin expression levels by virtue of adjusting specific activity, which can be exploited for visualization of low-level target expression or optimization of tumor-to-background contrast.

Keywords: positron emission tomography, receptor density, gallium-68, preclinical imaging

INTRODUCTION

The term "specific activity" (A_S) can refer to a variety of parameters, although its only meaning, by IUPAC definition, is "for a specified isotope, or mixture of isotopes, the activity of a material divided by the mass of the material" (*1*). In terms of radiolabelled compounds, A_S usually describes the activity of the radiolabelled compound divided by the mass of the radioactive and non-radioactive, cold reference compound, e.g. a small molecule, a peptide, an antibody fragment, etc. (*2*). In radiopharmaceutical sciences, all molecular species with comparable biological activity (e.g., affinity to a given receptor), are usually taken into account for the calculation of A_S, because the impact of A_S on biodistribution is governed by target saturation. This includes the radioactive and non-radioactive compound as well as similar species, such as the precursor or other non-separated species present in the preparation. Commonly used units are based on mass (e.g., MBq/µg) or molar amount (GBq/µmol, MBq/nmol), while mol-based units are to be preferred because they are more convenient for comparison of radiopharmaceuticals with different molecular weights regarding concentration-dependent effects, such as receptor saturation.

The impact of A_S on biodistribution, molecular imaging, and peptide receptor radionuclide therapy (PRRT) has been discussed repeatedly but, compared to other topics, rather infrequently. It is well known that a reduction of the A_S, for example, by deliberately increasing the concentration of all molecular species in the formulated solution that compete with the tracer for binding to the respective target ("excess

unlabeled"), can have a significant influence on the specific binding and thus overall pharmacokinetics of a radiopharmaceutical (*3*,*4*,*5*,*6*,*7*,*8*). However, possible implications for clinical practice are not yet fully investigated and understood (*9*). Presumably, the classic idea of the "radiotracer principle" (*10*), in its original form demanding application of tracers in lowest possible concentrations, has led to the still fairly popular notion that radiopharmaceuticals are ideally applied with the highest possible specific activity (*11*). On the other hand, it has been emphasized repeatedly that not only the administered amount of activity, but also, among various other parameters, a radiopharmaceuticals' mass dose is crucial for realization of truly personalized peptide receptor radionuclide therapy (PRRT) (*12*).

A strong influence of the amount of co-injected cold mass on tumor uptake has been demonstrated in a number of biodistribution studies on tumor xenografted rodents (*13*,*14*,*15*,*16*,*17*,*18*,*19*,*20*). As a general rule, it was found that tumor uptake increases with a decreasing total injected dose. For a variety of radiolabeled peptides a maximum is reached between 10 and 100 pmol per mouse (*13*,*14*,*15*,*16*,*17*,*18*). However, for very low doses (for example, <1 pmol of an ^{111}In-labeled exendin-3 targeting peptide (*14*), or ≤5 pmol of ^{111}In-DTPA-Phe^{1}-octreotide (*17*) or ^{67}Ga-labeled bombesin analog (*15*) per mouse), tumor uptake decreased again. At the same time, various patterns for the relation of A_S and uptake in non-tumor tissues have been observed for different radiopharmaceuticals, reaching from strong variation (*13*,*14*) to almost no influence of A_S (*16*,*17*,*18*,*19*).

Moreover, tumor-to-organ ratios frequently showed an optimum not at maximal but at intermediate specific activities. At this point, it appears logical that the target affinity will play a pivotal role as well, since at picomolar concentrations in vivo, a substantial degree of target binding should only be possible using tracers with picomolar affinities. Hence, application of high-A_S formulations for specific targeting of tissue areas with low receptor density should be strongly influenced, or even be made possible in the first place, by a high affinity of the tracer. However, to the best of our knowledge, a systematic experimental investigation of the mutual dependency of a radiopharmaceutical's A_S, its affinity, tissue receptor density, and observed uptake, has not been reported so far. Even complementary in-vivo images are scarce. Though some of the mentioned previous work also includes some single-photon emission computed tomography (SPECT) and PET scans, the knowledge potential of applying potent imaging agents with highly different A_S has not yet been explored systematically, most likely because minimal activities required for small-animal imaging are much higher than for biodistribution experiments. Particularly for PET-nuclides such as ^{68}Ga, limited A_S of tracers allowed for administration of very small mass doses only at the expense of very small activities, insufficient for high-quality imaging of rodents (*15*).

We recently introduced ^{68}Ga-Aquibeprin and ^{68}Ga-Avebetrin (formerly named ^{68}Ga-TRAP(RGD)$_3$) (*21*) for PET imaging of integrins $\alpha_5\beta_1$ and $\alpha_v\beta_3$, respectively (*22*). Due to their pronounced selectivity and virtually identical renal clearance kinetics, these radiopharmaceuticals allowed for complementary imaging of their respective target structures in the same tumor xenograft (M21 human melanoma, expressing

integrins $\alpha_5\beta_1$ and $\alpha_v\beta_3$) without interference. Both compounds are trimers (*23*) based on the TRAP (triazacyclononane-triphosphinate) chelator system (*24*,*25*) which possesses extraordinary affinity to (*26*,*27*,*28*) and selectivity for (*29*,*30*,*31*) gallium radionuclides. Therefore, ^{68}Ga-Aquibeprin and ^{68}Ga-Avebetrin can be routinely produced with very high A_S (*32*), enabling administration of activity doses sufficient for high-quality PET imaging (> 10 MBq) while injecting as little as single-digit picomolar amounts. In view of the aforementioned importance of high target affinity for tracers applied with high A_S, the compounds' high integrin affinities (^{68}Ga-Avebetrin: 190 pM, ^{68}Ga-Aquibeprin: 88 pM) (*22*) rendered them particularly suitable for a detailed investigation on the influence of specific activity on PET imaging contrast in mice.

MATERIALS & METHODS

General

Some of the applied experimental protocols have been fully described earlier, namely, ^{68}Ga labeling for rodent experiments (*21*), culture of M21 human melanoma cells, generation of respective xenografts in mice and their use in biodistribution experiments (*33*) as well as micro-PET imaging and immunohistochemistry (*22*). Descriptions of these protocols are provided in the Supplemental Information.

Radiochemistry

^{68}Ga-Aquibeprin (*22*) and ^{68}Ga-Avebetrin (*21*) were produced as described (*26*), yielding tracers with A_S of >1,000 GBq/µmol (typically 1,300–1,800 GBq/µmol, 30 min after start of elution). Lower A_S (or, more precisely, total injected amounts of biologically active compound) were adjusted by addition of unlabeled precursor (e.g., 0.15, 1.1, 7, or 55 nmol) to the injection syringes before administration. The actually injected total amounts of cold mass were calculated from syringe activities measured before and after injections. All data reported is based on mass doses; A_S values, given for orientation and comparison, are calculated for an exemplary activity dose of 20 MBq as administered for PET studies.

Biodistribution and PET studies

For general PET and biodistribution protocols, see Supplemental Information. For evaluation of specific activity-dependent uptakes in PET, volume regions of interest (ROIs) were drawn manually in the Siemens Inveon analysis interface for tumors, thigh muscle (two independent ROIs), kidneys (both), thyroid (^{68}Ga-Avebetrin only), both knee joints and both eyes (^{68}Ga-Aquibeprin only). Due to the comparably low resolution of ^{68}Ga-PET, individual ROIs for intra- and retroperitoneal organs (liver, stomach, spleen, pancreas, intestines) could not be reliably defined. In order to estimate gross organ uptake, a single ROI was drawn instead, covering the entire abdomen but excluding kidneys and urinary bladder. %ID/mL values were taken as calculated by the software.

RESULTS

Radiochemistry

^{68}Ga-Aquibeprin (*22*) and ^{68}Ga-Avebetrin (*21*) (for structures see Supporting Information) were obtained by fully automated ^{68}Ga labeling of 0.3 nmol of the respective precursors within 20 min, in approx. 95% decay-corrected yield. Since eluate fractions usually contained 600–800 MBq of ^{68}Ga at the start of syntheses, specific activities at the time of injection (25–40 min after start of syntheses; calculated by division of product yields by the total amounts of precursor, as described before) (*32*) were typically in the range of 1,300 to 1,800 MBq/nmol. For a typical activity dose of approx. 20 MBq administered for small-animal PET experiments, this was equivalent to 10–20 pmol of biologically active compound (taking into account all variations of starting activity, injected dose, and time between end of synthesis and tracer injection).

Lower specific activities over the range of 130 to 0.4 MBq/nmol could therefore be adjusted quite precisely by addition of comparably large amounts of unlabeled compound (150 pmol to 55 nmol) directly into the injection syringes. In order to improve precision, syringes were measured before and after injection, and the residual activities taken into account for determination of the total administered molar amounts.

Biodistribution

Ex-vivo biodistribution data was aquired 90 min p.i. for different total injected masses of compound (see Figure 1). Generally, uptake of ^{68}Ga-Avebetrin and ^{68}Ga-Aquibeprin in all organs and tissues is decreasing when increasing mass dose. However, this effect is more pronounced for ^{68}Ga-Aquibeprin, which shows particularly high uptakes at high specific activities >1,000 MBq/nmol, compared to those observed for 20 MBq/nmol. Kidney uptake of ^{68}Ga-Aquibeprin appears not to follow the strict pattern observed for all other tissues; however, such irregularities have been observed previously (*14*) and are most probably related to indeterministic variation of renal excretion.

Although tumor uptake of both radiopharmaceuticals is decreasing with a larger administered dose, tumor-to-tissue ratios show a remarkably different response. In case of ^{68}Ga-Avebetrin, the effect is somewhat inhomogeneous, although most tumor-to-tissue ratios are improving with lower A_S. In contrast, a much stronger and consistent influence of A_S on all tumor-to-tissue ratios is observed for ^{68}Ga-Aquibeprin. Figure 1 shows that the majority of the values reach an optimum for a dose of 6 nmol (approx. 3.5 MBq/nmol), where e.g. the tumor-to-muscle ratio peaks at 31.2 ± 5.4.

Interestingly, we observed an exceptionally high uptake of ^{68}Ga-Avebetrin in the adrenals (25.9 ± 7.7 % ID/g) for high specific activity (> 1000 MBq/nmol). With increasing mass doses, adrenal uptake is reduced to insignificance and thus, is considered integrin $\alpha_v\beta_3$ specific. Furthermore, we found a peculiar ^{68}Ga-Aquibeprin

uptake in the eyes (4.5 ± 1.2 % ID/g); insignificant uptake at higher doses again proves target specificity.

PET imaging

Static PET scans were recorded 75 min p.i. for 20 min, in correspondence to biodistribution experiments (90 min p.i.). ROIs were drawn only for distinct and recognizeable sites; due to the fairly low resolution of ^{68}Ga-PET and a pronounced partial volume effect, separate addressing of many small organs is not feasible anyway. This circumstance furthermore has to be considered during interpretation of the ROI-based uptake values for small hotspots, such as the eyeballs; a quantitative correlation with ex-vivo biodistribution is not to be expected here.

Notwithstanding this, the PET-based uptake data Figure 2) are well corresponding to actual visual contrast, and particularly the PET-derived tumor-to-tissue ratios (Figure 3) allow for a valid conclusion in terms of optimization of tumor imaging. In accordance with biodistribution experiments, decreasing uptake in the tumor as well as in other tissues is observed with decreasing specific activity (Figure 2). However, tumor uptake of ^{68}Ga-Aquibeprin remains at a high level (1.5 % ID/g) even upon administration of comparably large amounts of substance (6 nmol, ≈ 16 µg, specific activity: ≈ 3.5 MBq/nmol), which, in turn, already suppresses a large part of uptake in organs or muscle. As as result, tumor-to-muscle ratios are highest (12.4 ± 0.7) at this point (Figure 3), which is in accordance with biodistribution experiments. Surprisingly, tumor-to-background contrast is even better for a fairly large dose of ≈ 35 nmol (7.3 ± 0.4) than for < 20 pmol (5.3 ± 0.7).

For further illustration of these findings, Figure 4 shows ^{68}Ga-Aquibeprin PET images of three different M21-bearing SCID mice which were scanned up to three times, applying different doses. One immediately notices the intense ^{68}Ga-Aquibeprin uptake in the eyes at high A_S (dose of 14 pmol), which is almost completely disappearing when a ten-fold higher dose (140 pmol) is applied. A considerable uptake, similar for 14 and 140 pmol, is observed in the joints, which disappears using higher doses. Furthermore, despite a considerably lower tumor uptake for doses of 6 nmol, a low background activity provides excellent tumor-to-background contrast. Comparison of scans of different animals with the same specific activity demonstrates a good reproducibility and substantiates the decisive influence of A_S / applied doses on imaging results.

A comparable behaviour is observed for ^{68}Ga-Avebetrin. Figure 5 shows that although a lower A_S entails lower uptake in both organs and tumor, delineation of the M21 xenograft is improved. Similar to the observations made for eyes and joints with ^{68}Ga-Aquibeprin, a strong signal of ^{68}Ga-Avebetrin in the thyroid, observed for high A_S, is fading when using higher doses. Unfortunately, the close proximity of the adrenals to the kidneys do not allow for a clear delineation of these organs in the PET, rendering a visual assessment of the effects observed in the biodistribution infeasible.

Immunohistochemistry

In order to further elucidate the origin of the peculiar difference of the uptakes of ^{68}Ga-Avebetrin and ^{68}Ga-Aquibeprin in the adrenals observed for high A_S,

expression of the integrin subunits β_3 and $\alpha 5$ in this organ was investigated by immunohistochemistry. Figure 6 shows a strong membraneous and cytoplasmic β_3 integrin expression in the adrenal medulla. Only a faint expression is detected in the outer cortex. The X-zone is β_3 negative, apart from single thrombocytes wherein presence of β_3 is owing to integrin $\alpha_{IIb}\beta_3$ expression. These results were verified by computer-assisted image analysis, revealing an approx. 150 times higher number of positive pixels per mm^2 for β_3 vs. α_5 integrin within the adrenal medulla (2202550 vs. 14710). This is in agreement with the observation that adrenal uptake of ^{68}Ga-Aquibeprin is much lower than that of ^{68}Ga-Avebetrin.

DISCUSSION

Why preclinical imaging studies benefit from high A_S

Preclinical studies on dose-dependency of a radiopharmaceutical's biodistribution do not necessarily require tracers with ultra-high specific activity. Particularly nuclides with longer half-life and an efficient labeling chemistry (notably ^{111}In in connection with DTPA-conjugates) allow for investigation of very low (down to single-digit picomolar) doses, because even very small amounts of activity (down to tens of bequerels) can still be quantified reliably in excised tissues owing to the high sensitivity of common gamma counters. Imaging, however, is a different story, because for both PET and SPECT/scintigraphy, the minimally required activities are much higher. Although PET is quite sensitive, all common positron emitters possess rather short half-lives, effectively limiting the maximal duration of image acquisition and,

therefore, sensitivity. Collimator-based techniques, such as SPECT, inherently possess limited sensitivity due to a comparably poor photon yield. Despite this can be partly compensated by longer acquisition times due to longer half-lives of the respective nuclides, scan times for in-vivo imaging of rodents are furthermore restricted by anaesthesia and animal welfare considerations. Hence, in a common setting, application of e.g. 5–10 MBq of a PET nuclide, such as ^{68}Ga or ^{18}F, is considered adequate to obtain a decent in-vivo scan within reasonable time (< 30 min). In case of ^{68}Ga, this translates to A_S of 500–1,000 MBq/nmol for a dose of 20 pmol. For radiopharmaceuticals addressing saturable targets, such as peptide receptors, many interesting effects are observed for such or even lower doses (*14*,*15*). A_S of >500 MBq/nmol are, however, impossible to reach with most standard approaches, such as for ^{68}Ga-DOTA peptides (*32*). In contrast, ^{68}Ga-TRAP peptides like ^{68}Ga-Aquibeprin or ^{68}Ga-Avebetrin, can be obtained routinely with A_S up to 5,000 MBq/nmol and, under optimal conditions, >10,000 MBq/nmol (*32*), rendering them ideally suited for investigation of the effects of ultra-low dosage by PET imaging.

In this context, the scientific value of performing actual imaging deserves special attention. Biodistribution experiments inherently do not go beyond the intended area of investigation, because generation of data is restricted to the tissues collected. Unexpected effects, although potentially important, might be overlooked. This is exemplified by the case of ^{68}Ga-Aquibeprin imaging, where the peculiar uptake in the eyes at ultra-high A_S (Figure 4) was not addressed on purpose but discovered accidentally by PET imaging. For clinical translation of novel radiopharmaceuticals,

such observations nevertheless must be considered highly relevant, because common clinical doses of imaging agents are corresponding to ultra-low doses in mice (*4*). For example, assuming that ^{68}Ga-DOTATATE is typically applied with A_S in the range of 10–50 MBq/nmol, a typical dose (150 MBq ~ 3–15 nmol) in an average patient (70 kg) calculates to approx. 40–200 pmol per kg body weight, which is equivalent to a dose of 1–5 pmol for a mouse weighting 25 g. As long as the usual PET tracer production and dosage routines (i.e., the microdosing approach) are adhered to, effects observed in ultra-low dose rodent PET are therefore not an oddity but, on the contrary, should be expected to govern the observations made in the course of first-in-man applications. In other words, preclinical imaging using radiolabeled receptor ligands with ultra-high A_S is much more likely to actually correspond to clinical results.

Integrin $\alpha_5\beta_1$ / $\alpha_v\beta_3$ selectivity of ^{68}Ga-Aquibeprin and ^{68}Ga-Avebetrin

Angiogenesis (synonym: neovascularization) is a common feature of a variety of ophtalmic diseases and can occur in various functional compartments of the eye, such as the cornea, iris, retina, and choroid (*34*). In mice, strong expression of integrin $\alpha_5\beta_1$ was observed during corneal neovascularization, which could be inhibited by administration of a integrin $\alpha_5\beta_1$ antagonist (*35*). A comparable study in rats demonstrated that integrin α_5 is particularly expressed in distal areas where vessels are just about to develop, while integrin β_3 appears not to be involved in corneal neovascularization at all (*36*). Based on these findings, we assume that the strong ^{68}Ga-Aquibeprin signal in the eyes is indeed correlated to expression of integrin $\alpha_5\beta_1$, originating from neovascularization processes.

The strong immunohistochemistry signal for integrin β_3 in the adrenal medulla (Figure 6) is in accordance with a previous study on β_3 integrin gene expression (*37*). Since the β_3 subunit dimerizes with integrins α_v and α_{IIb}, a β_3 signal in thrombocytes is also found owing to expression of platelet integrin $\alpha_{IIb}\beta_3$, notwithstanding the fact that all other β_3 signals belong to actual $\alpha_v\beta_3$ expression.

Altogether, we assume that in the eye and the adrenals, only integrin $\alpha_5\beta_1$ and $\alpha_v\beta_3$, respectively, is present. A comparison of the uptakes of high-A_S ^{68}Ga-Aquibeprin and ^{68}Ga-Avebetrin (Supplemental Figure S2) in these organs thus further supports the finding that these radiopharmaceuticals possess complementary selectivity for their respective targets, as shown in previous study, wherein selectivity was proven by an invariant PET signal of either tracer in the $\alpha_5\beta_1/\alpha_v\beta_3$ expressing M21 tumor upon mutual cross-blockade with an excess of the respective other compound (*22*).

Impact of A_S on biodistribution and imaging contrast

Figure 1 and Supplemental Figure S2 furthermore show that high A_S resulted in a particularly increased uptake in tissues containing a lower absolute amount of receptors. While a change from high (> 1000 MBq/nmol) to intermediate A_S (20 MBq/nmol) entailed only a moderate decrease in M21 tumor uptakes of both ^{68}Ga-Aquibeprin and ^{68}Ga-Avebetrin (by 31 % and 43 %, respectively), ^{68}Ga-Aquibeprin uptake in the eyes dropped dramatically by 90 % from 4.5 ± 1.2 to 0.44 ± 0.05 % ID/g. Similarly, an exceptionally high uptake of ^{68}Ga-Avebetrin in the adrenals (25.9 ± 7.7 % ID/g) was reduced by 76 % to 6.2 ± 1.9 % ID/g, which is corresponding well to previously reported values (about 5 % ID/g) for radiolabeled RGD peptides (*38*,*39*). In

contrast, much lower uptake modulations are observed for ^{68}Ga-Avebetrin in the eye, and for ^{68}Ga-Aquibeprin in the adrenals, indicating that the observed effects are indeed related to the differences in target expression, and not to metabolism or unspecific accumulation.

The high accumulation of high-A_S ^{68}Ga-Avebetrin in the adrenal medulla furthermore suggests that administration of radiopharmaceuticals with high A_S / in low doses might be particularly useful for addressing such small tissue areas with high receptor expression density, since a much lower modulation of uptake by A_S is observed for large organs with low receptor density, e.g., the liver (*36*) (see Figure 1). Concerning uptake in adrenals, a similar observation has been made earlier upon variation of the amount of ^{111}In-DOTATOC administered to rats. For doses of approx. 300 and 30 pmol, uptakes of approx 1.6 and 8.3 % ID/g, respectively, were found (*13*), most likely mediated by somatostatin receptor expression on pheochromocytes located in the adrenal medulla. The dose range and extent of the A_S-dependent uptake variation observed for ^{68}Ga-Avebetrin and ^{111}In-DOTATOC is strikingly similar and suggests that both phenomena are essentially governed by the same principles.

However, we presently can not satisfyingly describe to which extent the high target affinities of the tracers (^{68}Ga-Avebetrin: 190 pM, ^{68}Ga-Aquibeprin: 88 pM) (*22*) are governing the A_S-related effects we observed, although we suspect a causal relationship. In an earlier study, biodistribution of ^{68}Ga-NOPO-RGD (an integrin $\alpha_v\beta_3$ targeted cyclo(RGDfK) monomer with a $\alpha_v\beta_3$ affinity of 1.0 ± 0.1 nM) was evaluated with high A_S (1500 MBq/nmol) in the same tumor model (*38*), but uptake in the

adrenals was only 5.2 ± 1.9 % ID/g (120 min p.i.). Despite there are a considerable number of pharmacological variables affecting the in-vivo behavior of compounds, we nevertheless assume that high affinity plays a decisive role here. We currently hypothesize that high uptake in small tissue compartments requires radiopharmaceuticals possessing both a high target affinity *and* high specific activity. This combination of properties might be key for effective PRRT of small-sized tumor lesions, such as micrometastases.

ACKNOWLEGDMENTS

Financial support by the Deutsche Forschungsgemeinschaft (grant #NO822/4-1 and SFB 824, projects Z1 and Z2), is gratefully acknowledged. The authors furthermore thank Sybille Reder, Markus Mittelhäuser and Marco Lehmann for assistance with small-animal PET; Martina Wirtz, Stephanie Robu and Monika Beschorner for assistance with animal experiments.

REFERENCES

1 van Grieken R, de Bruin M. Nomenclature for radioanalytical Chemistry. *Pure Appl Chem.* 1994:66;2513–2526.

2 Breeman WAP, de Zanger RMS, Chan HS, de Blois E. Alternative method to determine Specific Activity of ^{177}Lu by HPLC. *Curr Radiopharm.* 2015;8:119–122.

3 Lambert R, Willenbrock R, Tremblay J, et al. Receptor Imaging with Atrial Natriuretic Peptide Part 1: High Specific Activity Iodine-123-Atrial Natriuretic Peptide. *J Nucl Med.* 1994;35:628–637.

4 Kung MP, Kung HF. Mass effect of injected dose in small rodent imaging by SPECT and PET. *Nucl Med Biol.* 2005;32:673–678.

5 Sabet A, Nagarajah J, Dogan AS, et al. Does PRRT with standard activities of ^{177}Lu-octreotate really achieve relevant somatostatin receptor saturation in target tumor lesions?: insights from intra-therapeutic receptor imaging in patients with metastatic gastroenteropancreatic neuroendocrine tumors. *EJNMMI Res*. 2013;3:82. (full paper)

6 Breeman WAP, Kwekkeboom DK, Kooij PPM, et al. Effect of dose and specific activity on tissue distribution of indium-111-pentetreotide in rats. *J Nucl Med*. 1995;36:623–627.

7 Velikyan I, Sundin A, Eriksson B, et al. In vivo binding of [^{68}Ga]-DOTATOC to somatostatin receptors in neuroendocrine tumours—impact of peptide mass. *Nucl Med Biol*. 2010;37:265–275.

8 Velikyan I, Beyer GJ, Bergström-Pettermann E, Johansen P, Bergström M, Långström B. The importance of high specific radioactivity in the performance of ^{68}Ga-labeled peptide. *Nucl Med Biol*. 2008;35:529–536.

9 Hicks RJ. The difference between medicine and magic is that magicians know what they are doing. *Eur J Nucl Med Mol Imaging*. 2015;42:1–4.

10 Levi H. George Hevesy and his concept of radioactive indicators—in retrospect. *Eur J Nucl Med*. 1976;1:3–10.

11 Eckelman WC. True radiotracers: are we approaching theoretical specific activity with Tc-99m and I-123? *Nucl Med Biol*. 2008;35:523–527.

12 Beauregard JM, Hofman MS, Kong G, Hicks RJ. The tumour sink effect on the biodistribution of ^{68}Ga-DOTA-octreotate: implications for peptide receptor radionuclide therapy. *Eur J Nucl Med Mol Imaging*. 2012;39:50–56.

13 de Jong M, Breeman WAP, Bernard BF, et al. Tumour uptake of the radiolabelled somatostatin analogue [DOTA^0, TYR^3]octreotide is dependent on the peptide amount. *Eur J Nucl Med*. 1999;26:693–698.

14 Brom M, Oyen WJG, Joosten L, Gotthardt M, Boerman OC. ^{68}Ga-labelled exendin-3, a new agent for the detection of insulinomas with PET. *Eur J Nucl Med Mol Imaging*. 2010;37:1345–1355.

15 Schuhmacher J, Zhang H, Doll J, et al. GRP receptor-targeted PET of a rat pancreas carcinoma xenograft in nude mice with a ^{68}Ga-labeled bombesin(6-14) analog. *J Nucl Med*. 2005;46:691–699.

16 Froidevaux S, Calame-Christe M, Schuhmacher J, et al. A gallium-labeled DOTA-alpha-melanocyte-stimulating hormone analog for PET imaging of melanoma metastases. *J Nucl Med*. 2004;45:116–123.

17 Bernhardt P, Kölby L, Johanson V, Nilsson O, Ahlman H, Forssell-Aronsson E. Biodistribution of ^{111}In-DTPA-D-Phe1-octreotide in tumor-bearing nude mice: influence of amount injected and route of administration. *Nucl Med Biol*. 2003;30:253–260.

18 Konijnenberg MW, Breeman WAP, de Blois E, et al. Therapeutic application of CCK2R-targeting PP-F11: influence of particle range, activity and peptide amount. *EJNMMI Res*. 2015;4:47. (full paper)

19 Tolmachev V, Wållberg H, Sandström M, Hansson M, Wennborg A, Orlova A. Optimal specific radioactivity of anti-HER2 Affibody molecules enables discrimination between xenografts with high and low HER2 expression levels. *Eur J Nucl Med Mol Imaging*. 2011;38:531–539.

20 Tolmachev V, Rosik D, Wållberg H, et al. Imaging of EGFR expression in murine xenografts using site-specifically labelled anti-EGFR ^{111}In-DOTA-Z (EGFR:2377) Affibody molecule: aspect of the injected tracer amount. *Eur J Nucl Med Mol Imaging*. 2010;37:613–622.

21 Notni J, Pohle K, Wester HJ. Be spoilt for choice with radiolabelled RGD peptides: Preclinical evaluation of ^{68}Ga-TRAP(RGD)$_3$. *Nucl Med Biol*. 2013;40:33–41.

22 Notni J, Steiger K, Hoffmann F, et al. Complementary, Selective PET-Imaging of Integrin Subtypes $\alpha 5\beta 1$ and $\alpha v\beta 3$ Using Ga-68-Aquibeprin and Ga-68-Avebetrin. *J Nucl Med*. 2016;57:460–466.

23 Baranyai Z, Reich D, Vágner A, et al. A shortcut to high-affinity Ga-68 and Cu-64 radiopharmaceuticals: one-pot click chemistry trimerisation on the TRAP platform. *Dalton Trans*. 2015;44:11137−11146.

24 Notni J, Šimeček J, Wester HJ. Phosphinic acid functionalized polyazacycloalkane chelators for radiodiagnostics and radiotherapeutics: unique characteristics and applications. *ChemMedChem*. 2014;9:1107−1115.

25 Šimeček J, Wester HJ, Notni J. Copper-64 labelling of triazacyclononane-triphosphinate chelators. *Dalton Trans*. 2012;41:13803−13806.

26 Notni J, Šimeček J, Hermann P, Wester HJ. TRAP, a Powerful and Versatile Framework for Gallium-68 Radiopharmaceuticals. *Chem Eur J*. 2011;17:14718–14722.

27 Šimeček J, Schulz M, Notni J, et al. Complexation of Metal Ions with TRAP (1,4,7-Triazacyclononane-Phosphinic Acid) Ligands and 1,4,7-Triazacyclononane-1,4,7-triacetic Acid: Phosphinate-Containing Ligands as Unique Chelators for Trivalent Gallium. *Inorg Chem*. 2012;51:577−590.

28 Poty S, Désogère P, Šimeček J, et al. MA-NOTMP: A Triazacyclononane Trimethylphosphinate Based Bifunctional Chelator for Gallium Radiolabelling of Biomolecules. *ChemMedChem*. 2015;10:1475–1479.

29 Šimeček J, Zemek O, Hermann P, Wester HJ, Notni J. A monoreactive bifunctional triazacyclononane-phosphinate chelator with high selectivity for Gallium-68. *ChemMedChem*. 2012;7:1375−1378.

30 Šimeček J, Hermann P, Wester HJ, Notni J. How is ^{68}Ga-labelling of macrocyclic chelators influenced by metal ion contaminants in ^{68}Ge/^{68}Ga generator eluates? *ChemMedChem*. 2013;8: 95−103.

31 Máté G, Šimeček J, Pniok M, et al. The Influence of the Combination of Carboxylate and Phosphinate Pendant Arms in 1,4,7-Triazacyclononane-based Chelators on their ^{68}Ga Labelling Properties. *Molecules*. 2015;20:13112−13126.

32 Notni J, Pohle K, Wester HJ. Comparative gallium-68 labeling of TRAP-, NOTA-, and DOTA-peptides: practical consequences for the future of gallium-68-PET. *EJNMMI Res*. 2012;2:28. (Communication)

33 Pohle K, Notni J, Bussemer J, Kessler H, Schwaiger M, Beer AJ. ^{68}Ga-NODAGA-RGD is a suitable substitute for ^{18}F-Galacto-RGD and can be produced with high specific activity in a cGMP/GRP compliant automated process. *Nucl Med Biol*. 2012;39:777–784.

34 Adamis AP, Aiello LP, D'Amato RA. Angiogenesis and ophthalmic disease. *Angiogenesis*. 1999;3:9–14.

35 Muether PS, Dell S, Kociok N, et al. The role of integrin α5β1 in the regulation of corneal neovascularization. *Exp Eye Res*. 2007;85:356–365.

36 Zhang H, Li C, Baciu PC. Expression of Integrins and MMPs during Alkaline-Burn–Induced Corneal Angiogenesis. *Inv Ophtal Vis Sci*. 2002;43:955–962.

37 Le Gat L, Gogat K, van den Berghe L, et al. The β3 Integrin Gene is Expressed at High Levels in the Major Haematopoietic and Lymphoid Organs, Vascular System, and Skeleton During Mouse Embryo Development. *Cell Commun Adhes*. 2003;10;129–140.

38 Šimeček J, Notni J, Kapp TG, Kessler H, Wester HJ. Benefits of NOPO As Chelator in Gallium-68 Peptides, Exemplified by Preclinical Characterization of ^{68}Ga-NOPO-c(RGDfK). *Mol Pharm*. 2014;11:1687–1695.

39 Dumont RA, Deininger F, Haubner R, Maecke HR, Weber WA, Fani M. Novel ^{64}Cu- and ^{68}Ga-Labeled RGD Conjugates Show Improved PET Imaging of $\alpha_v\beta3$ Integrin Expression and Facile Radiosynthesis. *J Nucl Med*. 2011;52:1276–1284.

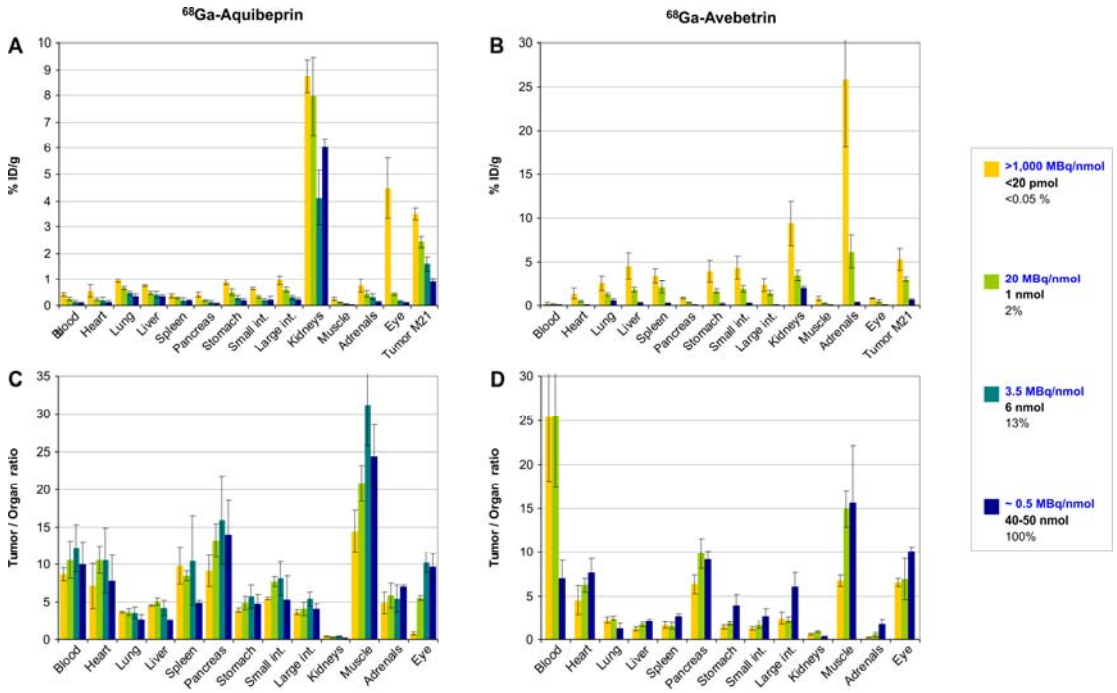

Figure 1: Biodistribution of ^{68}Ga-Aquibeprin (A,C) and ^{68}Ga-Avebetrin (B,D) in M21 xenografted SCID mice for different total injected molar amounts / specific activities (90 min p.i.), expressed as % injected dose per gram tissue (A,B) and tumor-to-organ ratios (C,D), data plotted as mean ± SD. Exact doses were 11.1 ± 7.7 pmol (n = 6), 0.98 ± 0.03 nmol (n = 4), 6.1 ± 0.4 nmol (n = 8), 51 ± 2 nmol (n = 4) for ^{68}Ga-Aquibeprin and 14.4 ± 5.3 pmol (n = 10), 0.99 ± 0.05 nmol (n = 5), 38 ± 3 nmol (n = 4) for ^{68}Ga-Avebetrin.

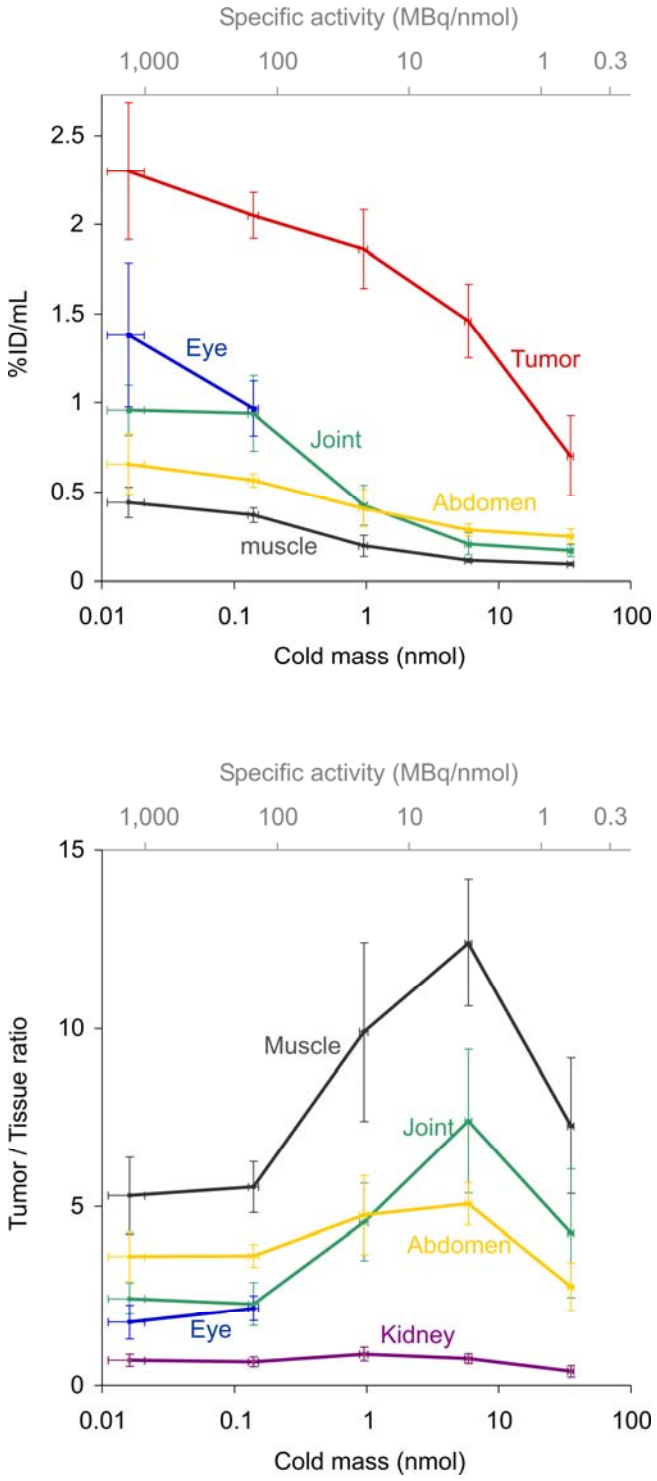

Figure 2: ^{68}Ga-Aquibeprin uptakes, expressed as % injected dose per mL (mean ± SD), and tumor-to-tissue ratios (mean ± SD) for different regions of interest as functions of injected total molar amount / specific activity (mean ± SD), derived from PET data (20 min static scans, 75 min p.i.; n = 3–8).

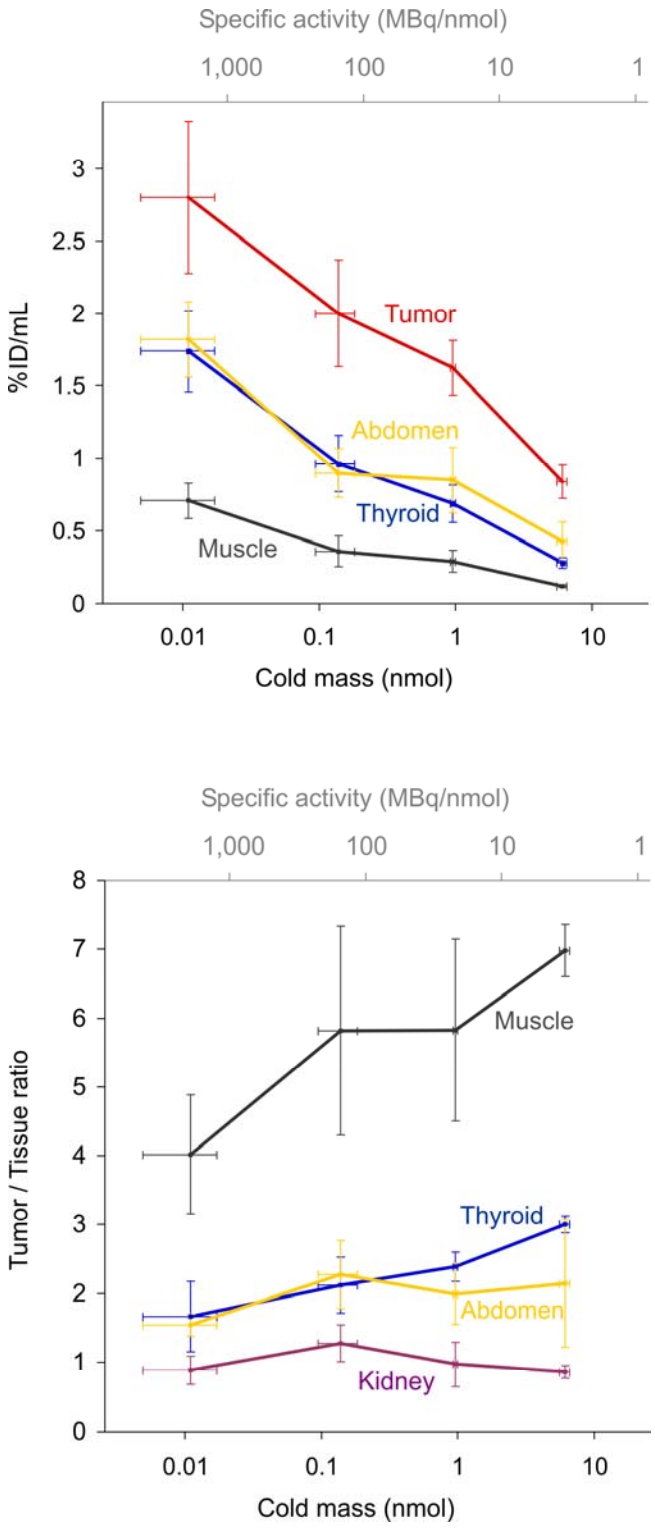

Figure 3: ^{68}Ga-Avebetrin uptakes, expressed as % injected dose per mL (mean ± SD), and tumor-to-tissue ratios (mean ± SD) for different regions of interest as functions of injected total molar amount / specific activity (mean ± SD), derived from PET data (20 min static scans, 75 min p.i.; n = 3–8).

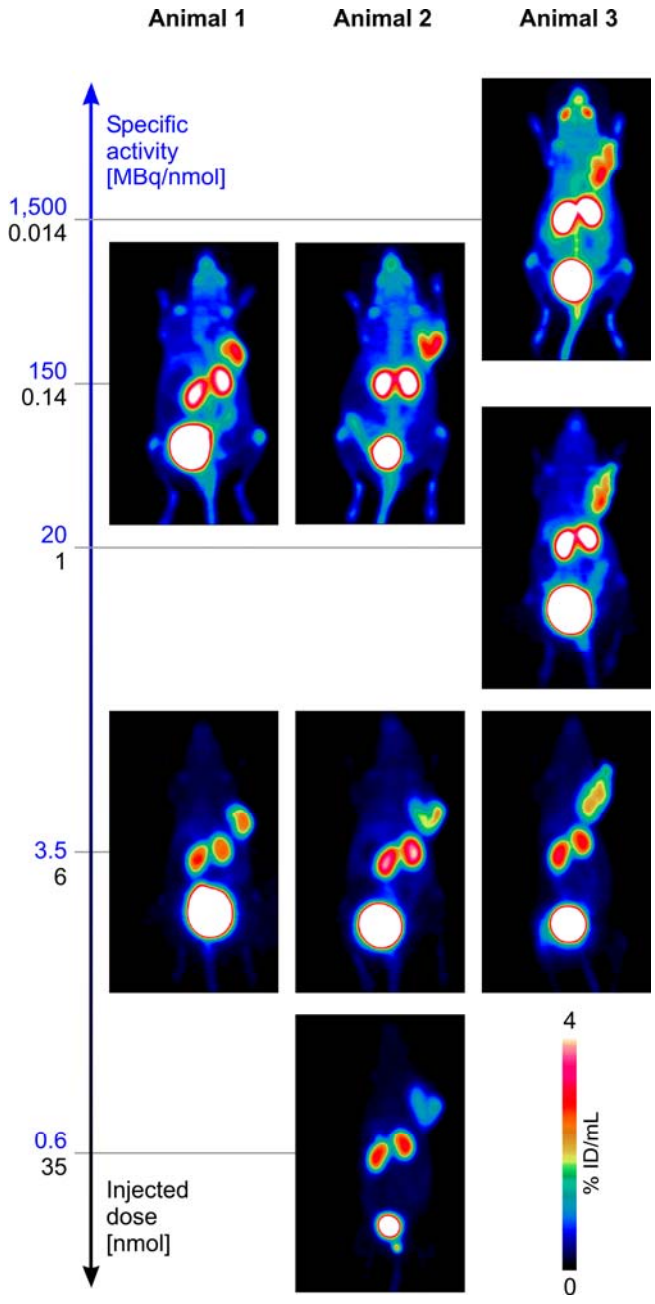

Figure 4: ^{68}Ga-Aquibeprin PET images (MIP, 15–20 MBq, 75 min p.i.) of three different SCID mice bearing M21 (human melanoma) xenografts on the right shoulder. Images belonging to the same animal are aligned vertically.

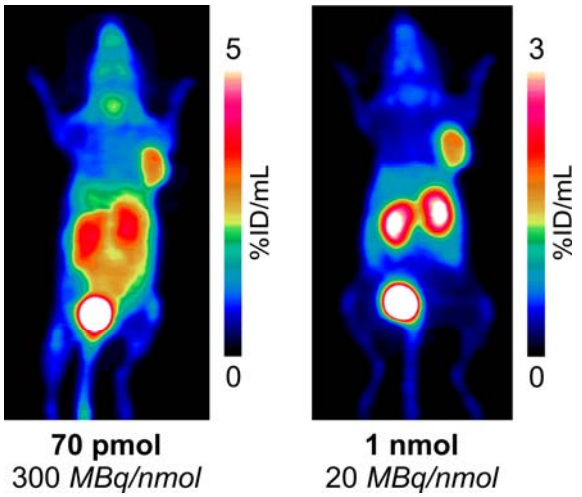

Figure 5: ^{68}Ga-Avebetrin PET images (MIP, 75 min p.i.) of the same M21 xenografted SCID mouse. Images are scaled to show the same visual intensity for the tumor, in order to highlight improved tumor-to-organ contrast using a higher mass dose. For images with the same scaling, see Supplemental Figure S1.

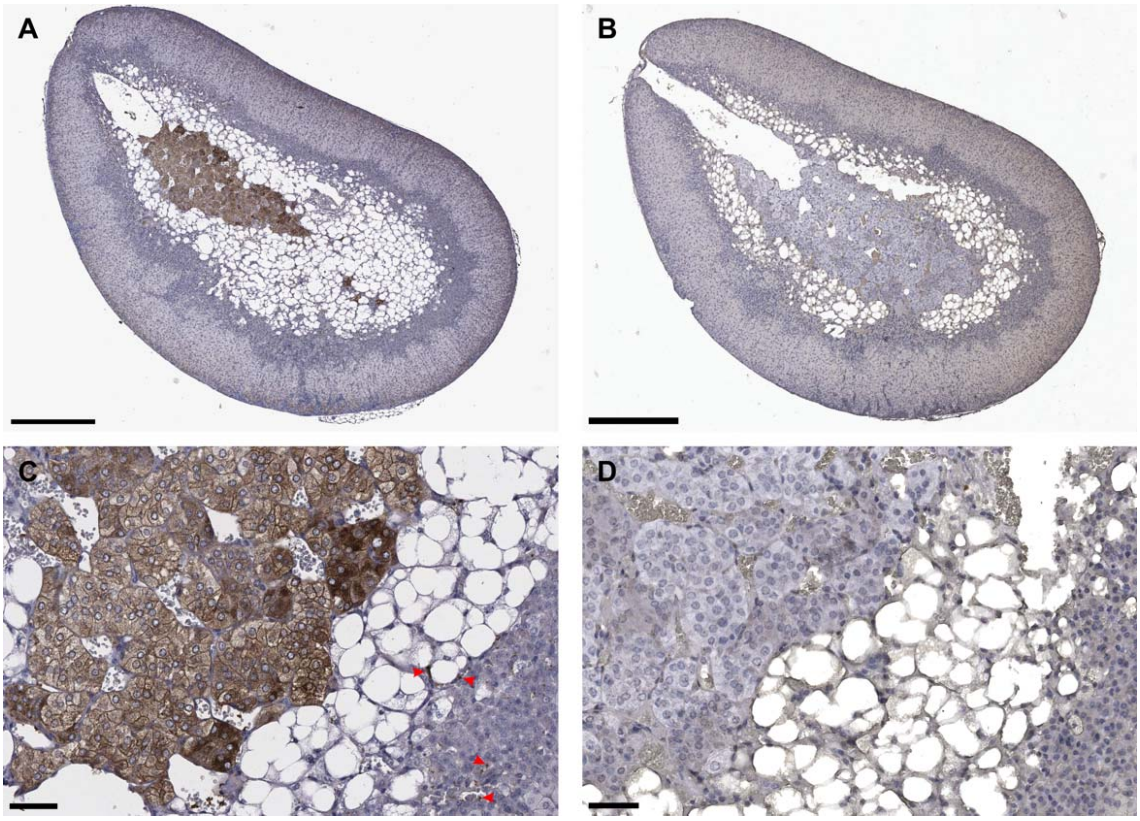

Figure 6: Immunohistochemistry of the adrenal gland, showing strong cytoplasmic and membraneous expression of integrin β_3 in the medulla (A, C) and in single trombocytes in the X-zone (C, examples marked by red arrowheads). No expression of integrin α_5 was detected (B, D). Scale bars indicate 500 µm (A, B) and 50 µm (C, D).